What is a flux tube? On the magnetic field topology of buoyant flux structures

Fausto Cattaneo

Department of Mathematics, University of Chicago, Chicago IL 60637

Nicholas H. Brummell, Kelly S. Cline[1]

JILA and Department of Astrophysical and Planetary Sciences, University of Colorado, Boulder CO 80309-0440

ABSTRACT

We study the topology of field lines threading buoyant magnetic flux structures. The magnetic structures, visually resembling idealised magnetic flux tubes, are generated self-consistently by numerical simulation of the interaction of magnetic buoyancy and a localized velocity shear in a stably-stratified atmosphere. Depending on the parameters, the system exhibits varying degrees of symmetry. By integrating along magnetic field lines and constructing return maps, we show that, depending on the type of underlying behaviour, the stages of the evolution, and therefore the degree of symmetry, the resulting magnetic structures can have field lines with one of three distinct topologies. When the x-translational and y-reflectional symmetries remain intact, magnetic field lines lie on surfaces but individual lines do not cover the surface. When the y symmetry is broken, magnetic field lines lie on surfaces and individual lines do cover the surface. When both x and y symmetries are broken, magnetic field lines wander chaotically over a large volume of the magnetically-active region. We discuss how these results impact our simple ideas of a magnetic flux tube as an object with an inside and an outside, and introduce the concept of "leaky" tubes.

Subject headings: MHD – Sun: interior – Sun: magnetic fields – Stars: spots

---

[1]Current address: Department of Mathematics, Carroll College, 1601 North Benton Avenue, Helena MT 59625

1. Introduction

One of the more remarkable features of the magnetic field at the solar photosphere is its degree of spatial intermittency (see e.g. Weiss (1994)). Magnetic flux often appears in the form of intense, isolated elements surrounded by flux free, or nearly flux free plasma. This observation, together with the fact that the solar plasma has high electrical conductivity and therefore the magnetic field is nearly frozen into the ambient fluid, has led to the development of the flux tube as a useful idealization of magnetic behaviour (Parker 1979). In an ideal flux tube, the magnetic field is entirely confined to a compact region, typically cylindrical in shape, and embedded in a field-free environment. Because of its simple geometrical structure and conceptual appeal, it is often easier to describe magnetic phenomena in terms of a flux tube or a collection of such objects than in terms of a continuous magnetofluid. Indeed, the flux tube idea is so useful and versatile that much of our present understanding of solar magnetic activity is formulated in the language of flux tube models (see e.g. Ossendrijver (2003) and references therein). One of the distinctive properties of an idealised flux tube is that it has well-defined inside and outside. This feature, together with the frozen-in condition, implies that fluid that is initially inside the flux tube should remain inside, and fluid that is initially outside should not be able to penetrate the flux tube except through the end-points or through small resistive effects. This property can be reconciled with the more fundamental description of magnetic elements in terms of continuous fields by assuming that the magnetic field lines form flux surfaces. Since flux surfaces are material surfaces in an ideal fluid, a closed flux surface also divides the volume into an inside and an outside with the fluid in the inside unable to escape. However, the existence of flux surfaces in magnetic systems is by no means a foregone conclusion. In fact, it is not generally known if flux surfaces are a generic property of magnetic structures, or if they are rare and only found in special, highly symmetric situations. Clearly, if flux surfaces are present then flux tube models provide a simplified but still realistic description. If, on the other hand, they are absent, a description in terms of flux tubes may be misleading. Of course, the flux tube description may remain useful even when flux surfaces are not present, provided that the field lines remain close to surfaces.

This distinction between systems with or without good flux surfaces is not just of academic interest, but can actually lead to very different models of magnetic field evolution. This point can be illustrated by considering a simple example. Let us suppose that at some initial instant an axisymmetric buoyant flux ring is released from the equatorial plane somewhere in the interior of an idealized stratified but non-rotating and non-convecting "Sun". One possible evolution is that the flux ring moves radially outward towards the surface in an axisymmetric fashion. If the ring has flux surfaces, the fluid inside the ring cannot escape, forcing the flux ring to expand as it rises. If the stratification is severe, as it is in the Sun,

the cross-section of the ring must become huge to maintain transverse mechanical equilibrium. One way around this paradoxical situation is to assume that the rise of the ring is not axisymmetric, and that an upwards bump (or "Ω loop") develops, with material from the looping region draining down to the lower parts to avoid the catastrophic expansion. However, another possibility would be to assume that the flux ring is not bounded by flux surfaces so that fluid within the structure can be readily exchanged with the external environment. In this case, provided that the structure is "leaky" enough, the ring could, at least in principle, rise axisymmetrically without any need to expand. The axisymmetric case is, of course, an extreme situation; in general one would expect the buoyant rise of a flux ring to be non-axisymmetric, in which case the amount of drainage required would depend on the "permeability" of the flux ring and how it entrains. Either way, it is of some importance to know whether flux surfaces exist.

Clearly, the existence of flux surfaces depends on circumstances. One would not expect to find flux surfaces in fully-developed MHD turbulence. On the other hand, there are cases where it *looks* as if flux surfaces exist, and the problem is then to ascertain whether the assumed surfaces are actually present. In the current paper, we study a simple system in which the combined effects of a localized velocity shear and magnetic buoyancy lead to the formation of isolated magnetic flux structures. The appearance of these structures is such as to invite a description in terms of flux tubes, i.e., magnetic structures *with* flux surfaces. However, as we will find presently, the situation is more complicated, and flux surfaces sometime exist and sometimes do not, depending on the parameters and stages of the evolution. The general feeling one gets from these results is that flux surfaces may not be as generic as is commonly, if implicitly, assumed.

2. Model and methods

The present objective is to study the geometry of field lines in a system where a simple-minded analysis would suggest that flux surfaces are present and therefore that the flux structures are flux tubes. To this end, we consider a simple system in which a localized velocity shear interacts with an externally-imposed weak poloidal magnetic field to form localized toroidal structures. In the stratified environment, these structure are subject to magnetic buoyancy which, in some cases, causes them to rise and eventually leave the region of the localized shear. Despite its simplicity, this system contains many of the dynamical ingredients believed to be important for magnetic field evolution at the base of the solar convection zone, and is capable of complex spatio-temporal behaviour. This system has been examined in some detail in a number of papers (Brummell, Cline, & Cattaneo 2002;

Cline, Brummell, & Cattaneo 2003a,b). We refer the reader to Cline, Brummell, & Cattaneo (2003a) (hereinafter known as CBC) for details of the mathematical formulation and method of numerical solution. We limit ourselves here to a brief discussion of the geometry and of the three characteristic dynamical regimes that will be used as the basis for the present study.

2.1. Formulation

We study the evolution of magnetic fields in a stably-stratified, compressible atmosphere, subject to a driven parallel shear flow. The problem is examined in a Cartesian domain with aspect ratio $x_m : y_m : 1$, with z increasing downwards. In this geometry, the x direction is considered to be toroidal and the y and z directions poloidal. We assume that the domain contains a perfect gas and that the specific heats c_p, c_v, dynamic viscosity μ, thermal conductivity K, magnetic diffusivity η and gravitational acceleration are finite and constant. The evolution of the velocity $\mathbf{u} = (u, v, w)$, magnetic field $\mathbf{B} = (B_x, B_y, B_z)$, density ρ, temperature T, and pressure p is then described by the compressible MHD equations (not reproduced here for brevity; see CBC for details). At the upper and lower boundaries, we impose stress-free, impenetrable velocity conditions, and require that the vertical gradient of the horizontal components of the magnetic field vanish. We impose a constant temperature on the upper surface and a fixed heat flux through the lower one. We assume periodic boundary conditions in the horizontal directions.

A forcing function $\mathbf{F}$ is included in the momentum equations, chosen to drive, in the absence of magnetic effects, a steady, stable target velocity profile $\mathbf{U}_0$. The chosen profile (Figure 1) contains shear in both the y and z directions: $\mathbf{U}_0 = (U_0, 0, 0)$ with $U_0(y, z) = P(z)\cos(2\pi y/y_m)$. Here, $P(z)$ is a polynomial function of z chosen so that the velocity is non-zero between two horizontal levels, $z_0 = 0.4$ and $z_1 = 0.95$, with maximum amplitude U_m at $z_v = (z_0 + z_1)/2 = 0.675$, joined smoothly to the surrounding quiescent layers. Since the nonlinear advective terms for this profile are identically zero, setting $\mathbf{F} = (F, 0, 0)$ with $F = -P_r C_k \nabla^2 U_0$ with no magnetic fields present, forces an initial condition $\mathbf{u} = 0$ to evolve to $\mathbf{U}_0$. Provided that U_m is not too large, this velocity profile is stable to hydrodynamic perturbations.

The atmosphere is initially in polytropic hydrostatic balance with polytropic index m, and is threaded by a uniform, weak, horizontal, poloidal (y-directed) magnetic field of strength B_0.

Under standard nondimensionalisation of the equations, a number of parameters arise that govern the problem: C_k is the thermal dissipation parameter (related to the thermal

conductivity, K), $P_r = \mu c_p/K$ is the Prandtl number, $\zeta = \eta c_p \rho_0/K$, and the Chandrasekhar number $Q = B_0^2 d^2/(\mu_0 \mu \eta)$, with μ_0 the magnetic permeability, measures the strength B_0 of this background magnetic field (although a related parameter appears explicitly in the equations, $\alpha = P_r \zeta Q C_k^2$). The other parameters are fixed: $\gamma = c_p/c_v = 5/3, x_m = y_m = 0.5, \theta = 2, m = 1.6$. These parameters, together with the P_r and C_k chosen, ensure that the Rayleigh number is large and negative, and thus that the system is stable to convective motions.

Related derivable quantities that describe the importance of the viscous, magnetic, and thermal diffusivities relative to advection, are the Reynolds number R_e, magnetic Reynolds number R_m, and the Peclet number P_e,

$$R_e \equiv \frac{U_f y_m \rho}{\sigma C_k} \tag{1}$$

$$R_m \equiv \frac{U_f y_m}{\zeta C_k} \tag{2}$$

$$P_e \equiv \frac{U_f y_m \rho}{\gamma C_k} \tag{3}$$

respectively.

The evolution equations are solved numerically using a hybrid pseudo-spectral/finite different scheme with spatial resolution of at least 64^3 (see CBC for details).

2.2. Geometrical considerations

The effect of the localized velocity shear is to stretch the weak poloidal field into two oppositely-oriented flux structures in the x (toroidal) direction. The evolution of these structures depends on the parameters, as we shall describe presently. The objective of this paper is to study the geometry of the magnetic field lines in order to establish to what extent these magnetic structures conform to our natural ideas of flux tubes. The basic building blocks for our discussion are the magnetic field lines, or integral lines on $\mathbf{B}$ defined by the relation

$$d\mathbf{X} \times \mathbf{B} = 0, \tag{4}$$

or equivalently

$$\frac{dX_i}{ds} = B_i(\mathbf{X}(s)), \qquad \mathbf{X}(0) = \mathbf{X}_0, \tag{5}$$

where the last expression defines the parametric representation in terms of s of the field line through the point $\mathbf{X}_0$. It should be noted that we examine the geometrical properties of the

vector field **B** frozen in time; the variable s should not be interpreted as time. The magnetic field, of course, evolves with time, but we are concentrating on its properties at a sequence of instants. The equations for the field lines were integrated using a fourth-order Runge-Kutta method with cubic interpolation to evaluate values of the magnetic field between the grid points of the original simulation.

Since the system is periodic in both horizontal directions x and y, it is also useful to construct return maps defined in terms of the successive intersections of the magnetic field lines with a reference vertical plane, typically either the $y = 0$ or $x = 0$ plane (maps M_x and M_y respectively). The sets that are invariant under the iterated action of this map are either sets of isolated points, or lines, or more complicated objects. Of particular significance for the present discussion are invariant lines, because they correspond to flux surfaces. In particular, any closed invariant line corresponds to a flux surface that encloses a volume, i.e., a surface with an inside and an outside. We note that if the evolution were ideal, the existence of a flux surface at one instant would guarantee its existence for all time. However, non-ideal effects can lead to reconnection with associated changes in field topology, and possibly the destruction of flux surfaces.

3. Results

3.1. General behaviour of the system

The system under study here exhibits three regimes of behaviour (I, II and III) that we distinguish in terms of the symmetry of the solutions. Regime I solutions, realised for sufficiently small magnetic Reynolds numbers, possess translational symmetry in x and reflectional symmetry in y about the vertical mid-plane ($y = y_m/2$). Regime I solutions consist of two steady toroidal magnetic structures of opposite polarity whose centres are located slightly above the region of maximum shear. In this configuration, buoyancy drives a slow poloidal circulation, so that advection of magnetic field balances resistive diffusion and the structures persist for all time. At higher R_m, Regime II solutions are found, where the y mirror symmetry is broken. The equilibrium is unstable and, since diffusion is no longer sufficient to retard the magnetic buoyancy, one of the magnetic structures rises. This disrupts the region of shear production below, enforcing amplification of the other structure. This oppositely-polarised toroidal structure then rises next, and the process repeats, creating a continuous cycle of emerging alternating-parity structures. If the kinetic Reynolds number is sufficiently high, Regime III solutions, where the x invariance is also broken, are found. Here, the rise of the structures is influenced by a secondary Kelvin-Helmholtz instability (induced by the magnetic field) that causes the structures to twist.

The three regimes of behaviour are illustrated in Figure 2 which shows volume renderings of the magnetic intensity and time traces of the peak velocity and toroidal magnetic field magnitude. In all three cases, the magnetic structures have the visual appearance of tubes in the volume renderings. It is tempting to associate surfaces of constant color in these visualizations with actual magnetic flux surfaces. However, as we shall see presently, volume rendering (and consequently isosurfacing or contouring), though being very useful visual tools, do not always give a good representation of the geometry of field lines.

3.2. Field geometry and flux surfaces

We now examine the geometry of field lines in each of the three regimes. It is instructive to examine the return maps defined along the two horizontal (periodic) directions; M_x is the return map induced by the magnetic field of an $x - z$ plane back onto itself and M_y is the similar map for a $y - z$ plane. The typical situation for regime I is shown in Figure 3. The first panel shows the successive iterates with respect to M_x of fifteen distinct points. In this case, each point is mapped back onto itself, i.e., the invariant subsets with respect to M_x are single isolated points. The projection of the field lines going through one of these points (in the region of shear at $z = z_v$) onto the plane $z = 0$ is shown in the fourth panel (Fig. 3*d*). It can be seen that the field line enters the domain (at the bottom, $y = 0$), is dragged a long distance (multiple x periods) in the negative x direction by the velocity field of the bottom half of the domain, and then is carried back exactly the same amount (due to the y symmetry) in the positive x direction in the second half, eventually to exit at precisely the same location as it entered. The invariant sets of the fifteen field lines with respect to the M_y map (Fig. 3*b*) are sets of points, with the number of points in each set depending on height. For example, the field line whose projection is shown in Figure 3*d* can be seen to cross the $x = 0$ plane sixteen times and therefore appears as a set of sixteen points in Figure 13*b*. The points in a set do not necessarily lie horizontally, since field lines threading through a dynamically-active region may be raised or lowered. Figure 3*c* shows the projection of the fifteen field lines onto a $y-z$ plane, illustrating this point. In this regime, all field lines lie on flux surfaces, but, due to the reflectional symmetry, individual field lines close on themselves, and therefore no single line covers a surface.

This should be contrasted with the typical behaviour for regime II, as illustrated in Figure 4. In this case, the y mirror symmetry has been broken, individual field lines typically do *not* close back onto themselves (Fig. 4*d*) and therefore map out an entire flux surface. Consequently, the invariant sets of the return maps M_x and M_y are lines and not isolated points (Figs. 4*a*, *b*). The invariant sets in the return map M_y in Figure 4*b* are now identical

to the projections of the field lines shown in Figure 4*c* since the x translational symmetry is preserved. It should be noted that surfaces on which the field lines do close back upon themselves still exist. However, this behaviour is not generic since it requires the average pitch angle of the field line to be rational. In general, one expects the average pitch angle on any randomly chosen (generic) surface to be irrational.

The evolution of the flux surfaces as the regime II instability proceeds through one cycle is exhibited in Figure 5. An interesting feature is already apparent, namely that the flux surfaces (upper panels) do sl not coincide with contours of B_x (lower panels). In fact, in general they do not even have the same topology, since the flux surfaces in the return maps never form closed loops. However, it is precisely these closed contours that correspond closely to our visual perception of the magnetic structure.

In regime III, where the x invariance is finally lost and all the symmetries of the solution are now broken, flux surfaces do not exist in the region of shear for a substantial fraction of the evolution cycle. Figures 6 and 7 show the return maps M_x and M_y together with the contours of B_x during the rise and subsequent decay of one twisted structure. It can be seen that as the cycle progresses and a twisted structure is formed, increasingly chaotic regions of field lines appear in the return maps (Fig. 6). When the structure decays and before the next one forms, the regions of chaoticity in the maps decrease (Fig. 7). It should be noted that at the time of Figures 7*a*, *d*, *e* (which also corresponds to the volume rendering seen in Figure 2*c*), a substantial fraction of the domain volume does not contain any flux surfaces. Although the volume rendering gives the impression of two distinct magnetic structures, in actual fact field lines follow complicated trajectories visiting large portions of both structures and the surrounding regions. Thus, any fluid element initially inside one of the magnetic structures can end up in the interior of the other structure by moving entirely along a field line. In this sense, the magnetic structures are "leaky", without a well-defined inside and outside.

From Figures 7*a*, *d*, for example, it is clear that a chaotic field line can visit a large fraction of a volume. However, it is not apparent from this figure how many iterations of the map are needed for any given field line to wander a substantial distance. For instance, if the successive iterates remain close together in the map so that it takes many iterations to fill a substantial fraction of the plane, then, even though formally no flux surfaces exists, the flux structure is not very permeable. To explore this issue, we consider five iterations of the M_y return map acting on a set of points that are initially inside one of the closed contours (in B_x) delineating the rising magnetic structure. The results of this procedure are shown in Figure 8. At the end of the first iteration, the mapped points are still close to where they originated; at the end of the second, they have been displaced substantially but

they are still within the same magnetic structure; by the third iteration, many of the points have migrated to the other magnetic structure; and by the fourth iteration, they are widely scattered.

We can quantify the separation rate for trajectories by defining Lyapunov exponents for M_y by

$$\lambda_1(\mathbf{a}) = \frac{1}{n} \ln \Big(\frac{|\delta^n \mathbf{r}(\mathbf{a})|}{|\delta \mathbf{r}(\mathbf{a})|} \Big), \tag{6}$$

where

$$\delta^n \mathbf{r}(\mathbf{a}) = M_y^n \delta \mathbf{r}(\mathbf{a}), \tag{7}$$

and $\delta \mathbf{r}(\mathbf{a})$ is a small displacement vector in the $y - z$ plane centered at $\mathbf{a}$ and M_y^n represents the action of M_y iterated n times[2]. This construct then measures the rate of separation of points when acted on by successive iterations of M_y. The results of this calculation for the magnetic field in Figure 2*c* (and the map in Fig. 7*d*) are shown in Figure 9. It can be seen that there is a large area encompassing the shear layer, and thus the strongly magnetized region, where the Lyapunov exponent is substantial. It should be noted that the average value of the exponent quoted in Figure 9 is computed as an average over the entire plane; an average over the strongly chaotic regime gives a value of approximately 0.3, corresponding to an e-folding rate of once every three returns.

4. Conclusion

We have examined the geometry of field lines in a system where strong toroidal magnetic structures are spontaneously generated by the interaction of a localized velocity shear with a weak background poloidal magnetic field. Our objective was to establish whether magnetic surfaces exist in such a system. The existence of closed flux surfaces, which are required to define the inside and outside of structure, is commonly, if implicitly, assumed in many simplified models of magnetic structure evolution. We have found that, in this system, flux surfaces only exist in highly symmetric cases, and that for cases with no symmetry, no flux surfaces are present in the regions occupied by the magnetic structures. Furthermore, when flux surfaces are not present, the magnetic structures are quite "leaky", in the sense that the "outside" and the "inside" can readily communicate.

[2]Strictly speaking the orientation of the infinitesimal vector should be chosen so as to maximize the ratio (6). In practice, the vector quickly becomes aligned with the direction of largest stretching so that a formal maximization is not required.

It is natural to speculate about the existence of flux surfaces in more general systems and, in particular, in structures that arise naturally in the solar interior. In addressing this question, we note that the problem discussed in this paper is very laminar; the background environment is not turbulent and the Reynolds numbers of the induced flows are moderate. Even so, the generic behavior was such that the magnetic structures had no flux surfaces. This suggests that the chance of finding flux surfaces in the highly turbulent solar environment are slim, unless the dynamics surprisingly conspire to enforce a high degree of symmetry. However, the more basic issue for constructing meaningful models is not whether flux surfaces exist, but rather whether the associated magnetic structures are very permeable or not. This requires a detailed knowledge of the geometry of field lines, as provided here, for instance, by the Lyapunov exponents. Determination of such quantities for realistic solar situations is challenging, but should nevertheless be addressed.

We acknowledge useful discussions with David Hughes and Steve Tobias. This paper was completed whilst FC and NHB were attending the Magnetohydrodynamics of Stellar Interiors workshop at the Isaac Newton Institute, Cambridge, England. We thank the staff of the INI and the organisers of the workshop, Profs. David Hughes, Robert Rosner and Nigel Weiss, for their support and interaction. This work was supported by NASA Solar Physics Supporting Research and Technology grants to the Universities of Chicago and Colorado. KSC was also supported by a National Science Foundation Graduate Fellowship during this project.

REFERENCES

Brummell, N. H., Cline, K. S., & Cattaneo, F. 2002, MNRAS, 329, L73

Cline, K. S., Brummell, N. H., & Cattaneo, F. 2003, ApJ, 588, 630

Cline, K. S., Brummell, N. H., & Cattaneo, F. 2003, ApJ, 599, 1449

Ossendrijver, M. 2003, Astron. Astrophys. Rev., 11, 287

Parker, E.N. 1979, Cosmical Magnetic Fields, (Oxford: Clarendon)

Weiss, N. O. 1994, in Lectures on Solar and Planetary Dynamos, ed. M. R. E. Proctor & A. D. Gilbert, (Cambridge: Cambridge Univ. Press), 59

This preprint was prepared with the AAS LaTeX macros v5.2.

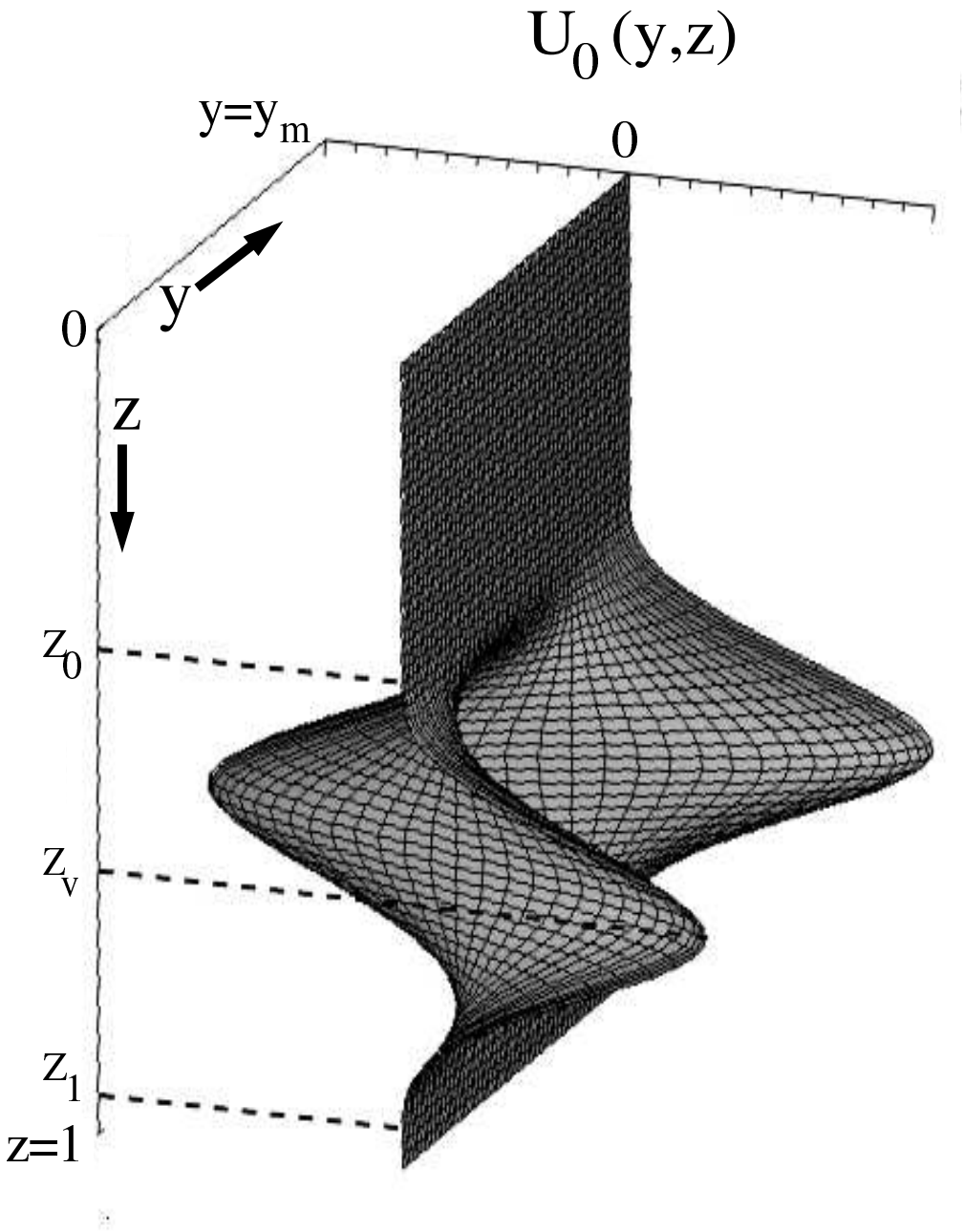

Fig. 1.— The target shear velocity profile $U_0(y, z)$. In the absence of magnetic effects, the forcing **F** drives this stable shear flow. The fluid in the upper and lower parts of the domain is at rest, and the shear is localized to a region in the lower portion of the layer.

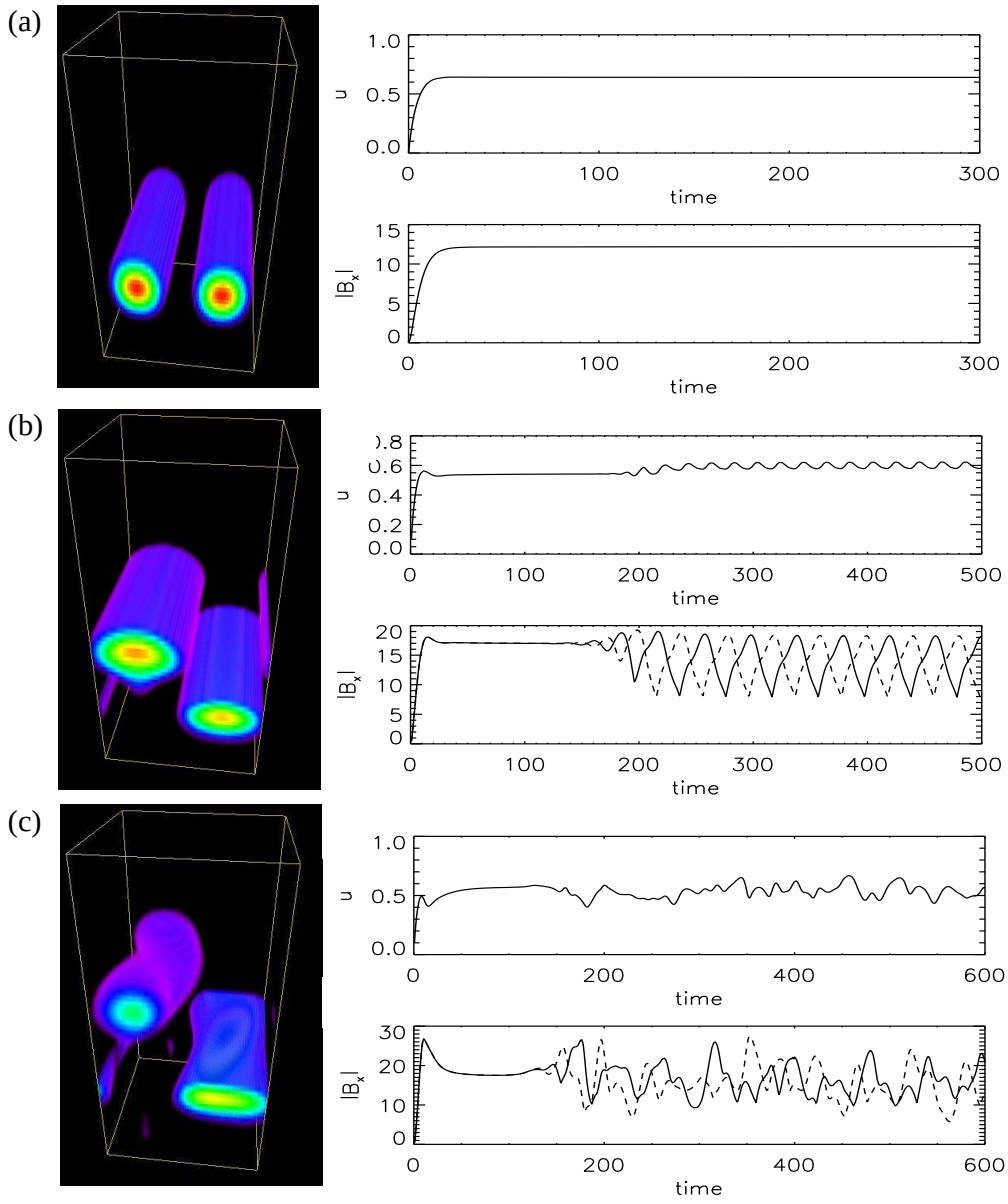

Fig. 2.— The generic classes of behaviour of the system. Shown are volume renderings of the magnetic intensity (where increasing intensity ranges through the colour sequence purple-blue-green-yellow-red and from translucent to opaque), together with time traces of the peak values of the x-directed velocity, u, and magnetic field, B_x (where peak values of positive B_x are the solid lines, and peak values of $|B_x < 0|$ are dashed). The volume renderings show a representative time in the evolution. (a) Regime I: the equilibrium state, with both translational symmetry in x and reflectional symmetry about the mid-y plane. (b) Regime II: found at higher R_m, the reflectional symmetry is broken, and alternately-directed magnetic structures emerge cyclically. (c) Regime III: found at higher $R_e e$, the x symmetry is broken by a magnetically-induced Kevin-Helmholtz instability that creates twisted magnetic structures.

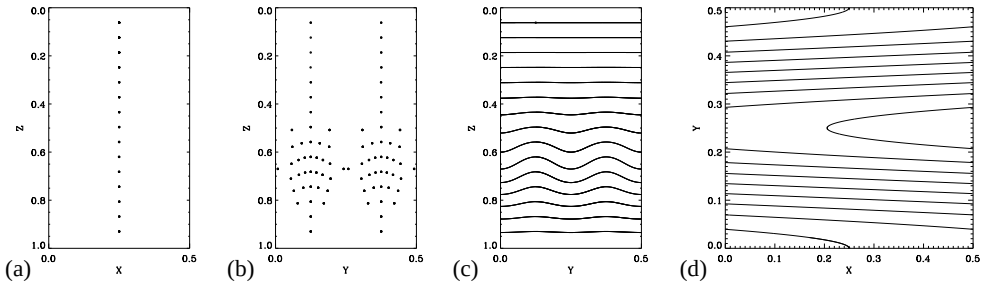

Fig. 3.— Return maps and projected field lines for the equilibrium case, regime I. (a) The return map M_x for fifteen field lines initiated at evenly spaced intervals in the vertical at $x = 0.25$. (b) The corresponding M_y map for the same field lines. (c) The projection of the same field lines onto the $y - z$ plane. (d) The projection of the single field line at height $z = z_v$ onto the $x-y$ plane. The invariant sets under M_x are individual points. The invariant sets under M_y are groups of points, where the number in a group depends on height. Field lines connect back on themselves and so it takes an infinite number of lines to map out a plane.

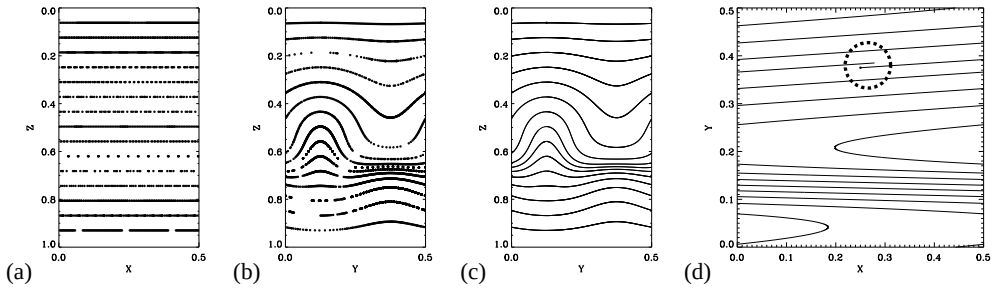

Fig. 4.— Return maps and projected field lines for the cyclically emerging state, regime II. The panels are the same as in Fig. 3. The invariant sets of both M_x and M_y are now lines, since, with the loss of reflectional symmetry, field lines no longer close back on themselves (as emphasised by the circle in (d)) and therefore cover an entire flux surface.

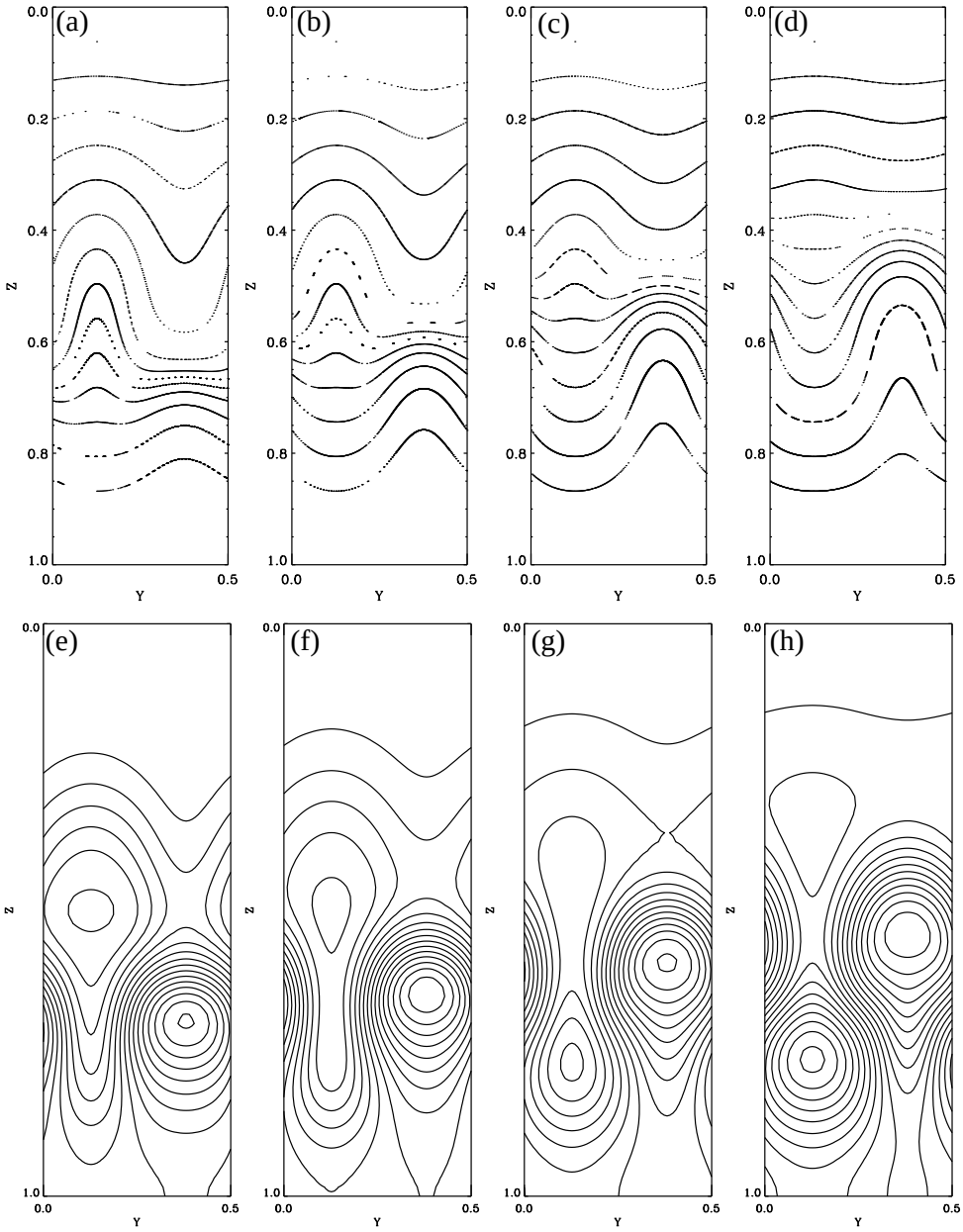

Fig. 5.— The time dependence of the map M_y for regime II. Panels $(a)-(d)$ show the map M_y at various snapshots throughout the cycle found in this regime, and panels $(e)-(h)$ show contours of B_x at the corresponding times. The invariant sets of the map remain as lines at all times, and show little correspondence with the closed contours defining the magnetic structure in B_x.

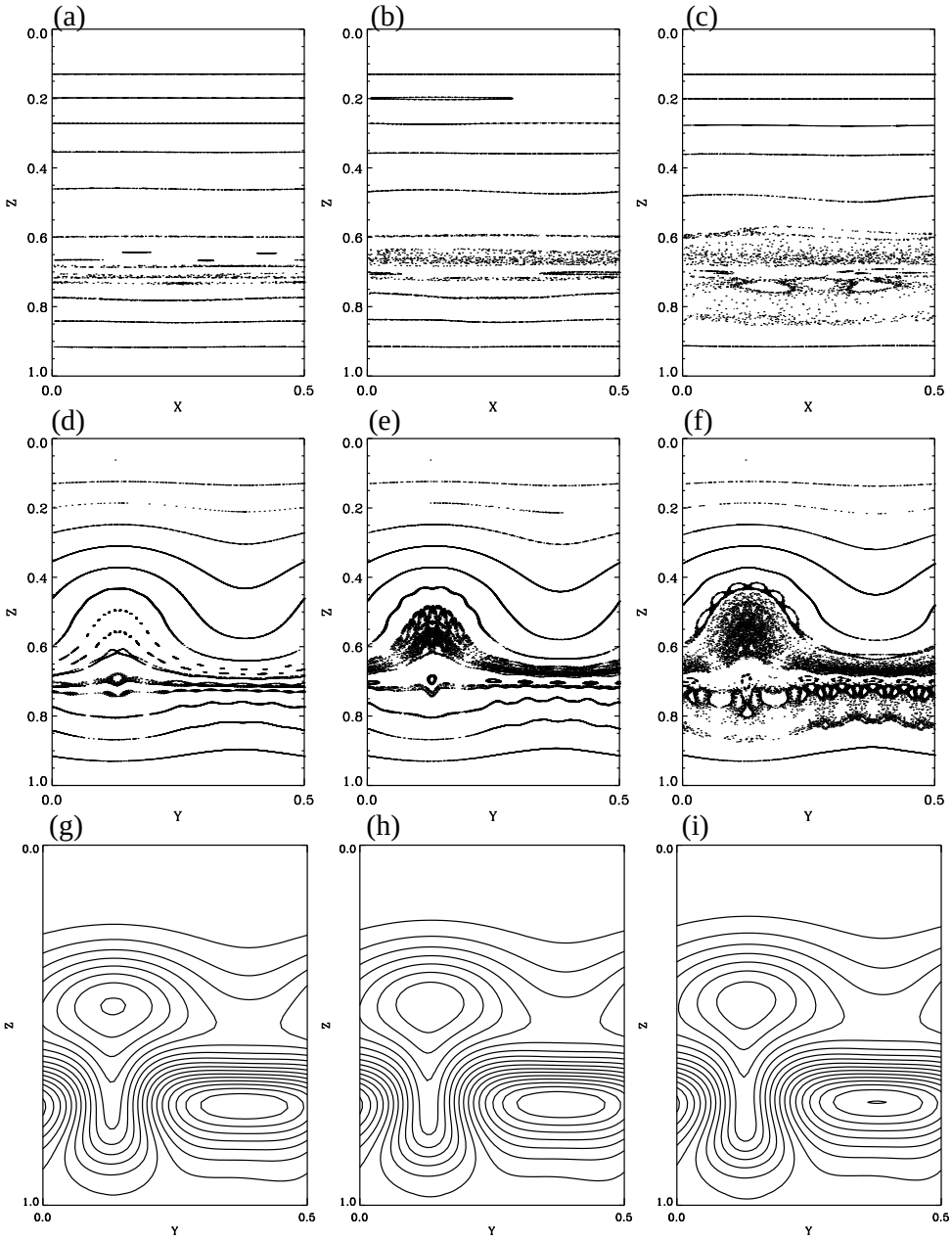

Fig. 6.— The time dependence of the maps M_x and M_y for regime III behaviour. Panels $(a)-(c)$ show M_x, panels $(d)-(f)$ show M_y, and panels $(g)-(i)$ show contours of B_x, for three times respectively during the formation, rise and twist (by Kelvin-Helmholtz modes) of a magnetic structure in this regime. The invariant sets of the maps are close to planes initially, but then the sets related to field lines that traverse the three-dimensional structure of the twisted tube expand to create complicated sets occupying an area. Some field lines wander chaotically through a substantial volume in the system. In the region where a magnetic structure is clearly delineated by the closed contours of B_x, no flux surfaces can be identified.

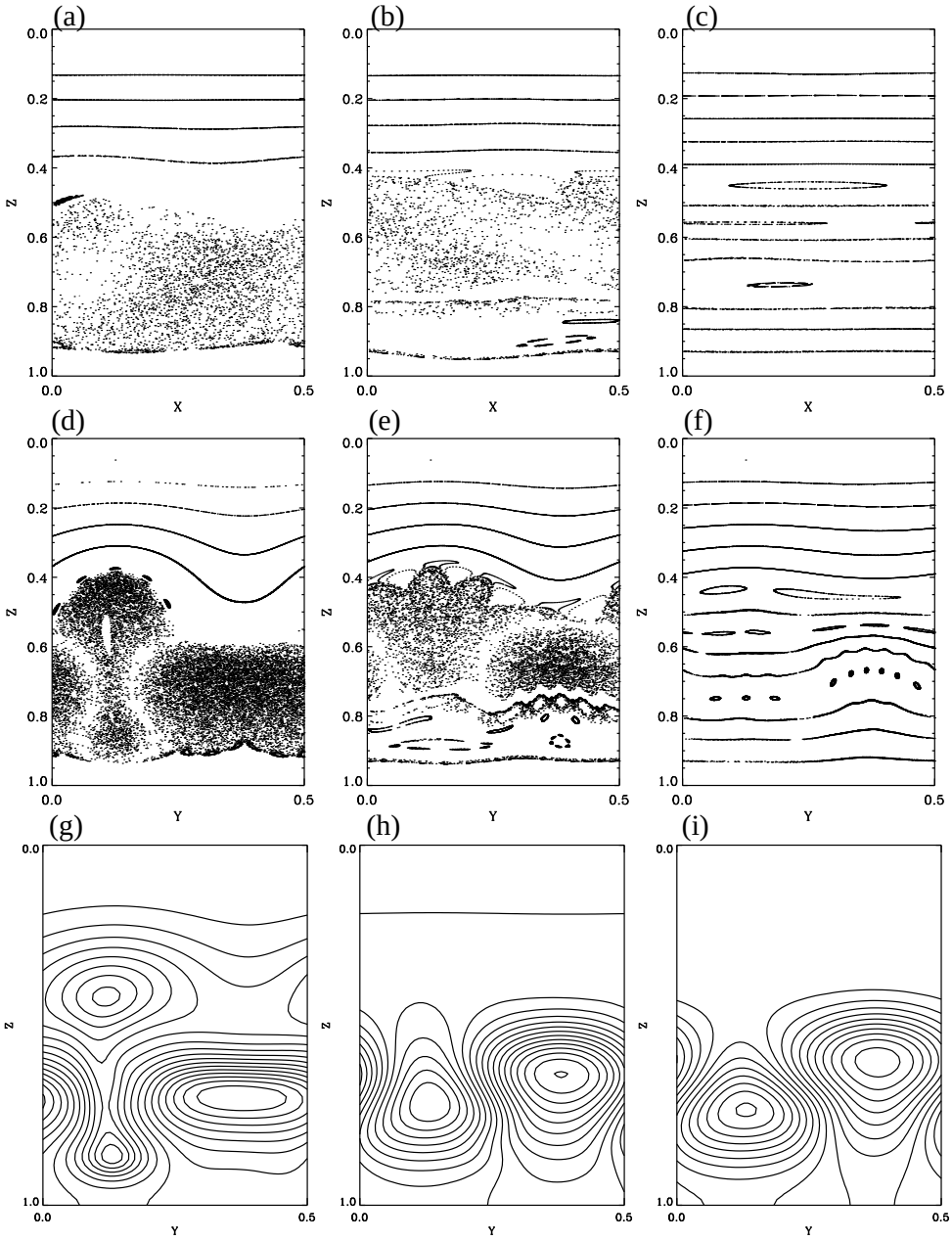

Fig. 7.— Continuation of Fig. 6 to show further time-dependence of M_x and M_y for regime III. Fig. 6 is extended with three subsequent times during the Kelvin-Helmholtz twist and then decay of a magnetic structure. Panels (a), (d), (g) show particularly clearly that the loss of all symmetries in the system has led to the existence of field lines that wander chaotically throughout the region of magnetic activity. As the three-dimensionality of the structures is eroded during their diffusive decay, the system tends back towards a state close to the regime II behaviour, and the invariant sets in M_x and M_y collapse back towards lines.

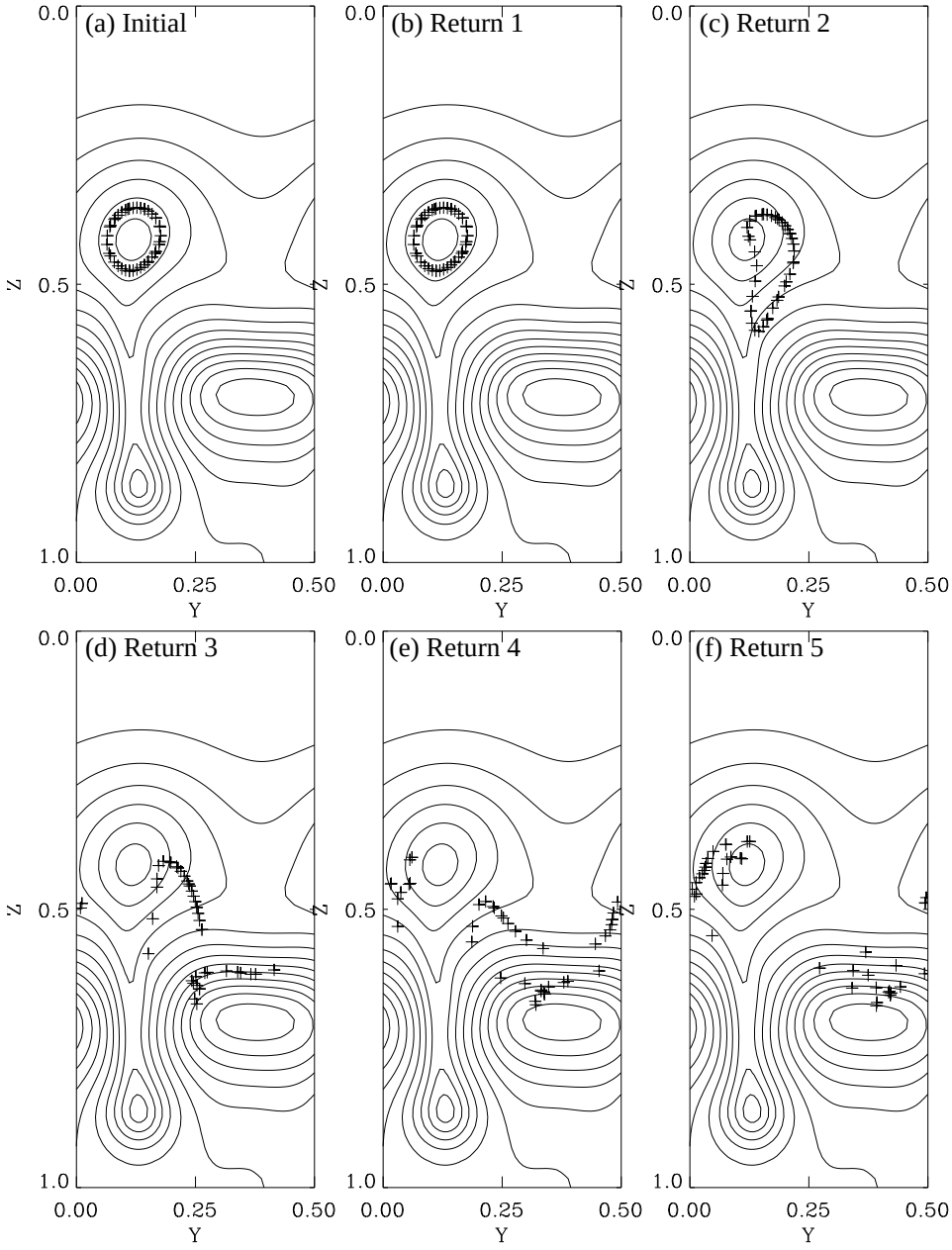

Fig. 8.— Five iterations of the return map M_y for the regime III twisted structure that produces Fig. 7(d). A set of field line initial positions are chosen within the closed contours of $B_x(z = 0)$ so that they may be considered "inside" the magnetic structure. The map is iterated five times and the subsequent returns plotted. It can be see that even after a small number of iterations, the field lines have wandered substantially outside of the obvious magnetic structure.

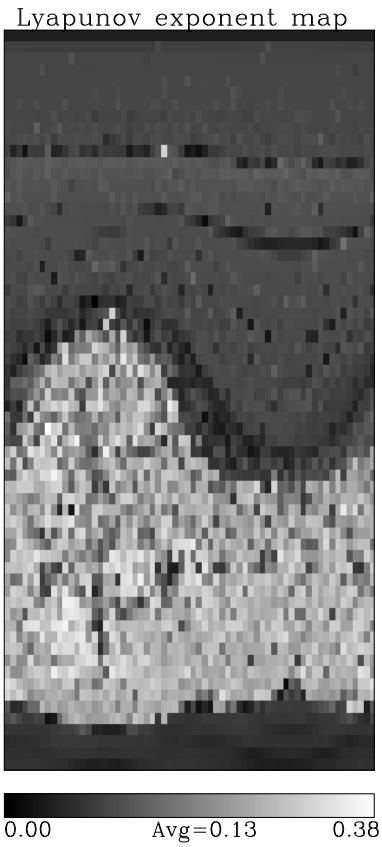

Fig. 9.— A grey-scale plot of the values of the Lyapunov exponents (representing the rate of exponential divergence of the field lines) against position for the system during the three-dimensional phase of regime III. The same time snapshot is used as was for Fig. 7(d) and Fig. 8. The region of magnetic activity is filled with large values of the exponent, averaging about 0.3, confirming the visual inference of Fig. 8 that merely three returns produce a substantial wandering of the trajectories field lines.